An NMR view of nonlinear magnetization dynamics: in liquid and solid, at low and high polarizations

Daniel Abergel
Laboratoire des biomolécules, CNRS/ENS/SU

From the nonlinear dynamical systems theory to observational chaos
October 9-11, 2023, Toulouse

Some context: nuclear spins in a magnetic field

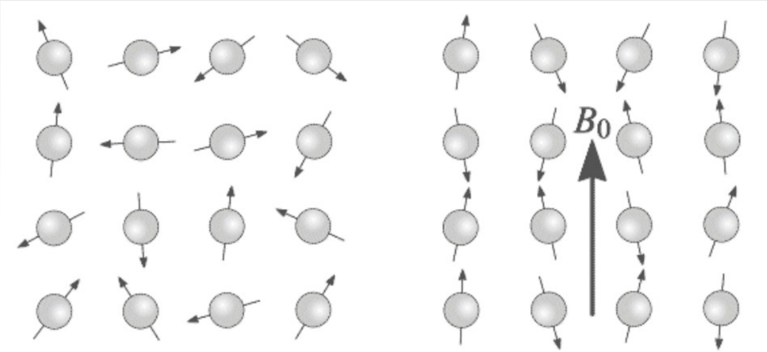

- Unequally populated energy levels lead to a macroscopic magnetization
- Energies in the radiofrequency range (~ 100-1000 MHz)
- Low polarizations for achievable fields and temperatures

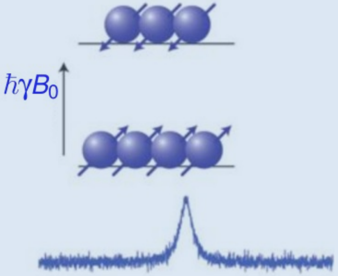

For spins $1/2$

$$P = \frac{n_+ - n_-}{n_+ + n_-} = \tanh \frac{\gamma\hbar B_0}{2k_B T}$$

$$M_z^{eq} \propto \gamma\hbar P$$

B_0 (T)	6.7	9.4	14.1
$T = 300$ K	2.3×10^{-5}	3.2×10^{-5}	4.8×10^{-5}
$T = 1.2$ K	5.7×10^{-3}	8×10^{-3}	12×10^{-3}

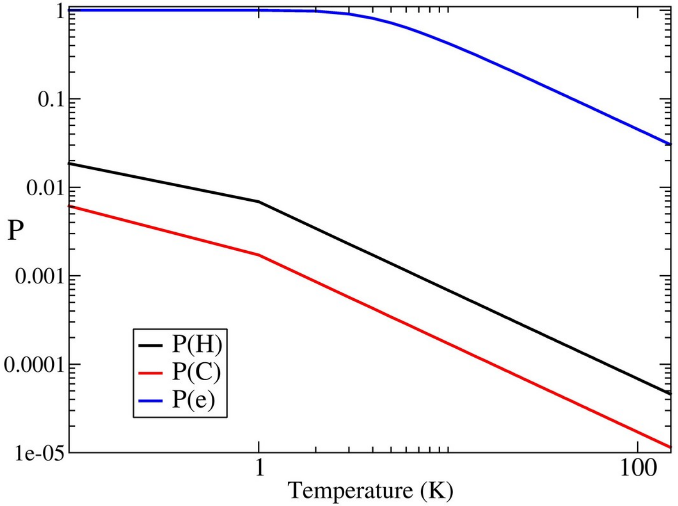

Classical dynamics of a magnetization in a magnetic field

$$\frac{d}{dt}\mathbf{M} = \gamma \mathbf{M} \times \mathbf{B}$$

Precession about a static $\mathbf{B}_0$

Angular frequency $\omega_0 = -B_0/\gamma$

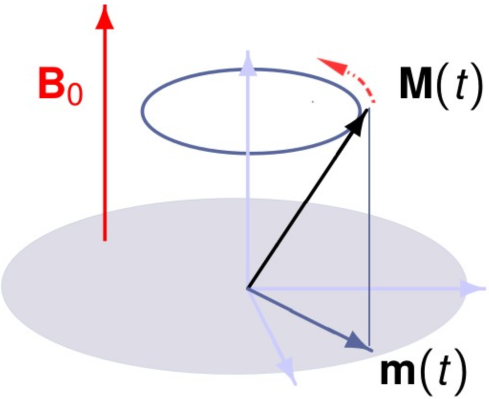

Classical dynamics of a magnetization in a magnetic field

$$\frac{d}{dt}\mathbf{M} = \gamma \mathbf{M} \times \mathbf{B}$$

Additional rf field

$$\mathbf{B}_1(t) = B_1(\cos\omega t)\mathbf{i} + \sin\omega t)\mathbf{j})$$

$$\left(\frac{d\mathbf{M}}{dt}\right)_{rf} = \gamma \mathbf{M} \times \mathbf{B}_{eff}$$

$$\mathbf{B}_{eff} = -\omega_1/\gamma\mathbf{i} - (\omega_0 - \omega)\mathbf{k}$$

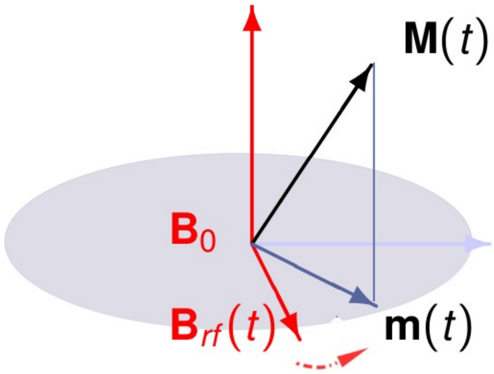

$$\left(\frac{d\mathbf{M}}{dt}\right)_L = \left(\frac{d\mathbf{M}}{dt}\right)_{rf} + \boldsymbol{\omega} \times \mathbf{M}$$

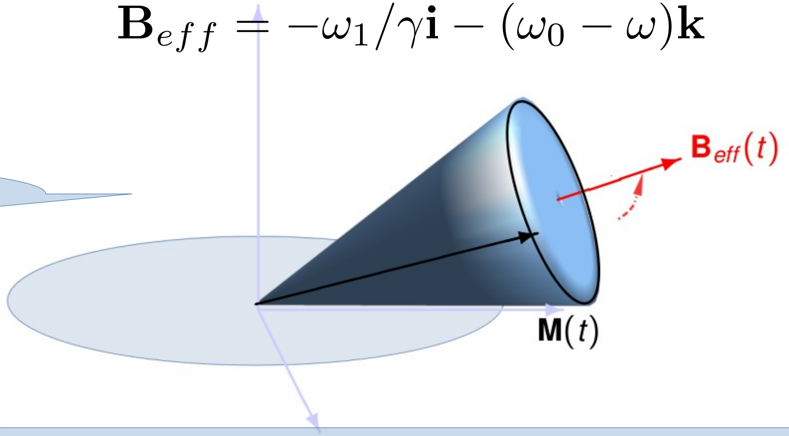

In this frame the field is time independent and the motion is simpler

Lab frame

Rotating frame

Classical dynamics of a magnetization in a magnetic field - Magnetic Resonance

$$\left(\frac{d\mathbf{M}}{dt}\right)_{rf} = \gamma \mathbf{M} \times \mathbf{B}_{eff}$$

$$\mathbf{B}_{eff} = -\omega_1/\gamma \mathbf{i} - (\omega_0 - \omega)\mathbf{k}$$

$$\omega = \omega_0 \Rightarrow \mathbf{B}_{eff} = B_1 \mathbf{i}$$

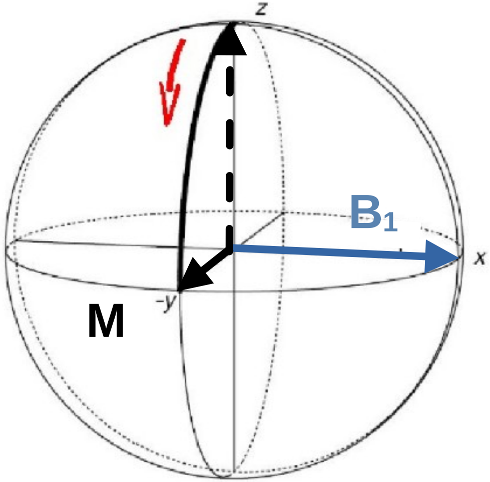

Magnetic resonance

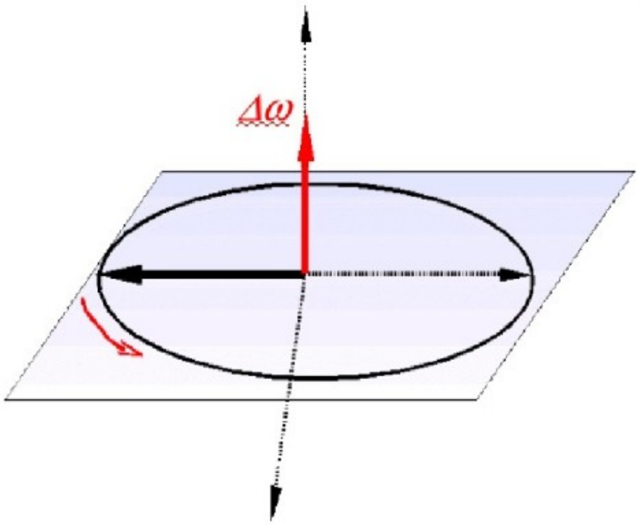

Precession about B_1 in the r.f.
If at $t=0$ $M//B_0$: magnetization vector set in motion and precesses in the xOy plane at ω_1

When B_1 is turned off, precession is about B_0

NMR detection: the induction signal

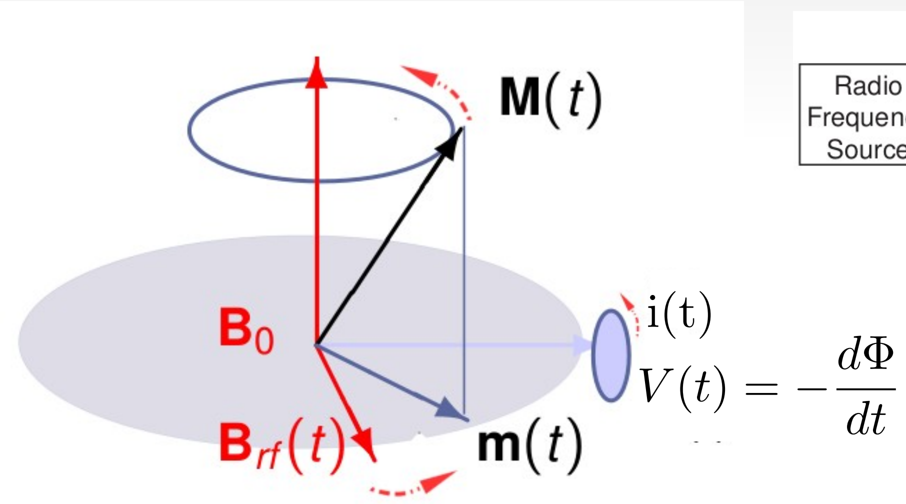

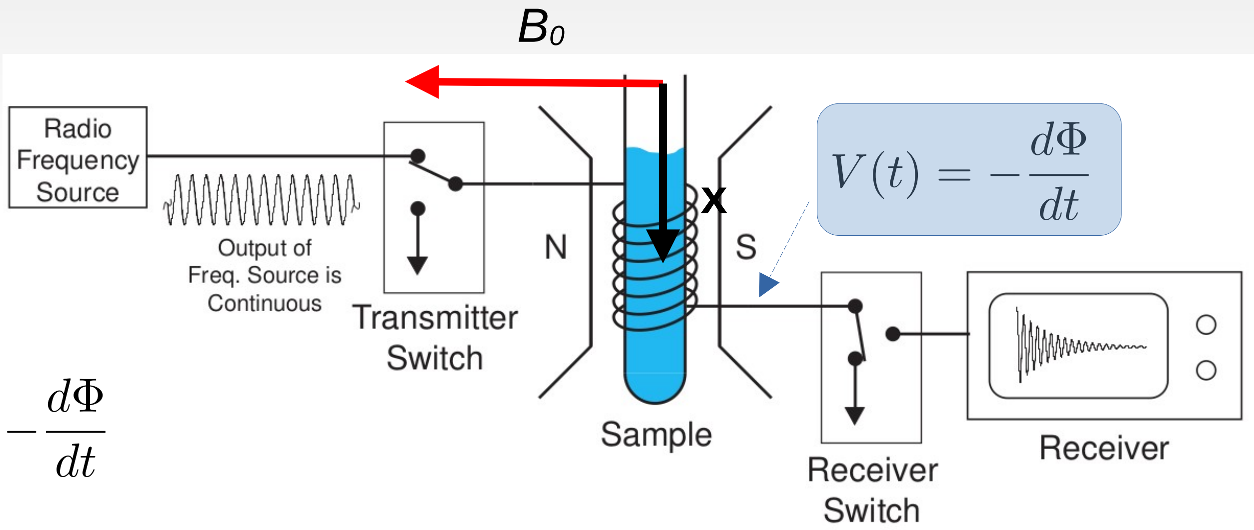

- The detecting coils are sensitive to the flux changes in the xy plane only
- Signal is produced by the transverse component of the magnetization

Classical magnetization dynamics: the Bloch equations

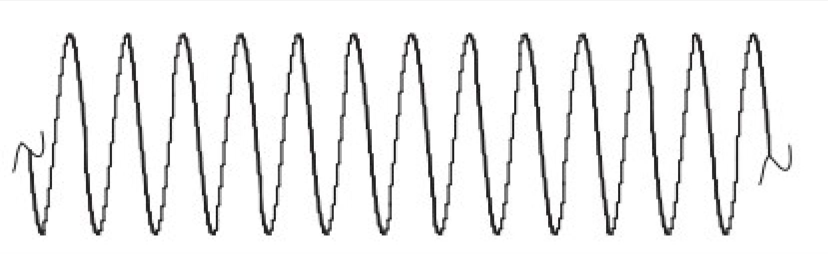

S(t) = sine wave

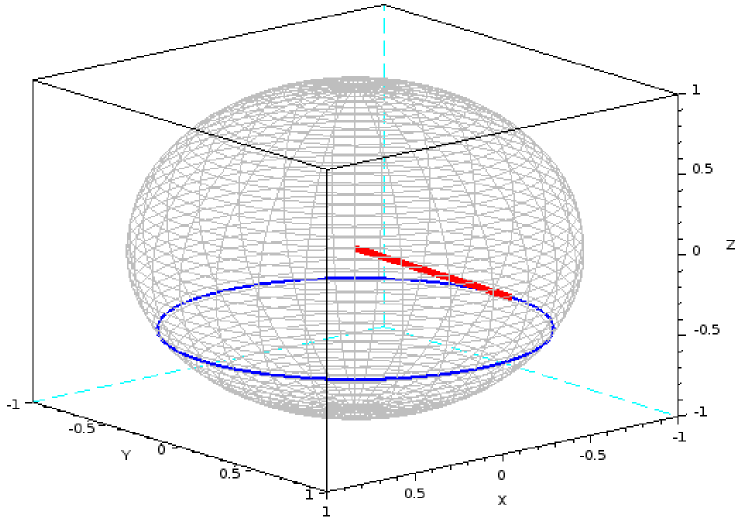

$$\frac{d}{dt}\mathbf{M} = \gamma \mathbf{M} \times \mathbf{B}$$

Classical magnetization dynamics: the Bloch equations

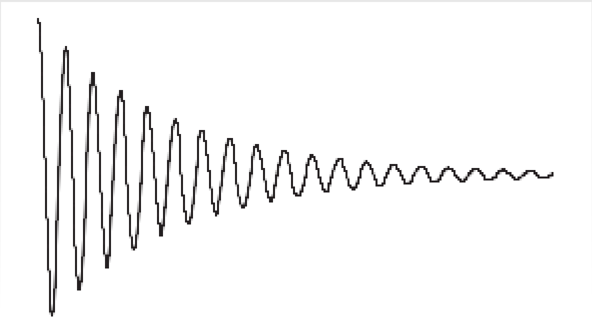

The actual signal is exponentially damped

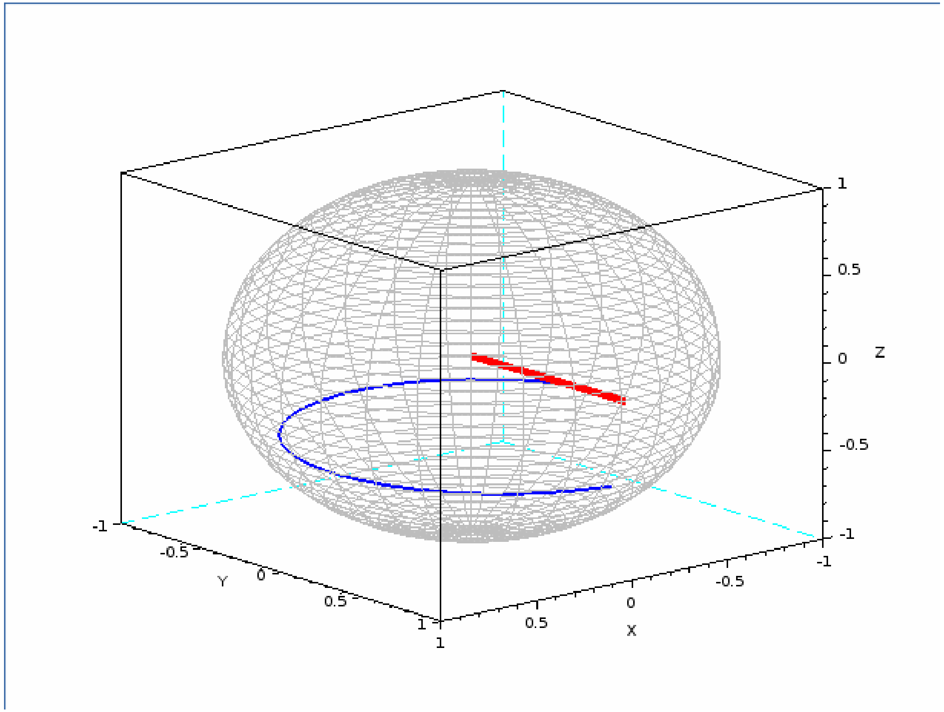

$$
\begin{aligned}
\frac{d}{dt}\mathbf{m} &= \gamma \mathbf{m} \times (\mathbf{B}_0 + \mathbf{B}_1(t)) - \gamma_2 (m_x \hat{\mathbf{x}} + m_y \hat{\mathbf{y}}) \\
&- \gamma_1 (\mathbf{m}_z) - \mathbf{m}_{oz}^{th}(t))\hat{\mathbf{z}}
\end{aligned}
$$

exponential return to equilibrium with γ_1

exponential damping with γ_2

Coupling of the precessing magnetization with the detecting circuit: the “radiation damping”

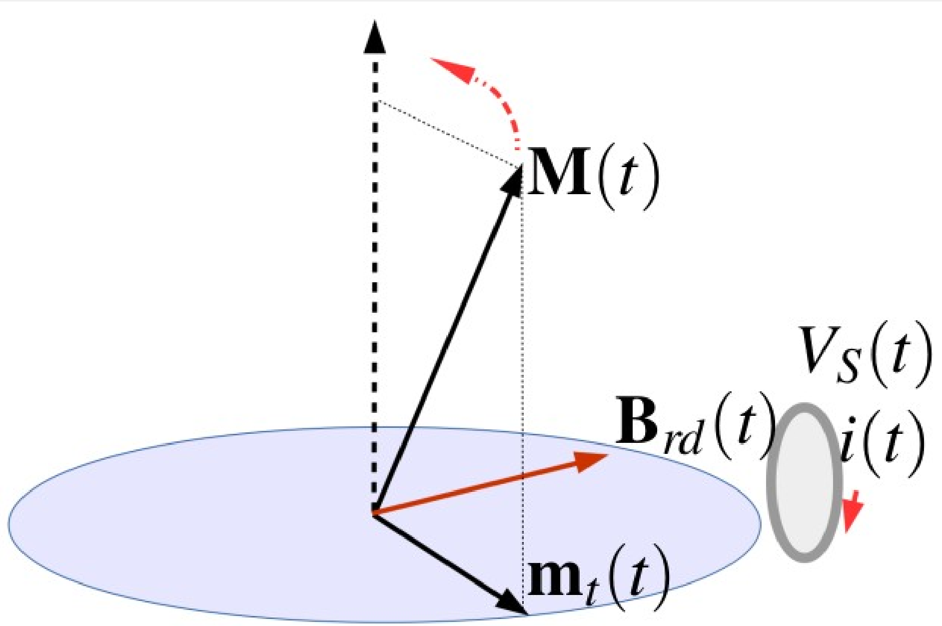

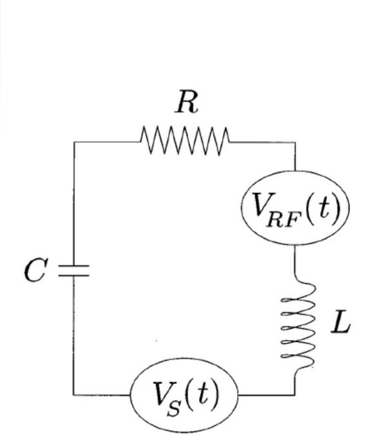

$$L\frac{d^2}{dt^2}i(t) + R\frac{d}{dt}i(t)i(t) + \frac{1}{C}i(t)dt = \frac{d}{dt}V_s(t)$$

$$V(t) = -\frac{d\Phi}{dt} \Rightarrow i(t) \Rightarrow \mathbf{B}_{rd}(t)$$

- For large magnetizations and moderately lossy circuits the coupling with the detecting circuit is efficient
- A significant feedback field is generated by the precessing magnetization

RD leads to nonlinear equations for the magnetization and a non exponentially decaying NMR signal

$$\begin{cases} \dfrac{d}{dt}M_x = -\delta\omega\tilde{M}_y - \gamma G M_x M_z \\ \dfrac{d}{dt}M_y = \delta\omega\tilde{M}_x - \gamma G M_y M_z \\ \dfrac{d}{dt}M_z = \gamma G (M_x^2 + M_y^2) \end{cases}$$

no relaxation: $\gamma_1, \gamma_2 = 0$

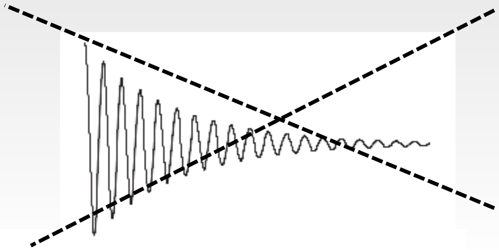

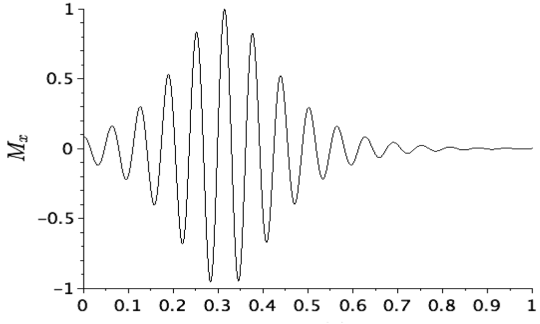

$$\gamma G = \frac{\mu_0 \eta Q}{2}$$

$$\mathrm{M}_t = M_0 \; sech \left(\tfrac{t-t_0}{\tau} - \log \left[\tan \tfrac{\theta(t_0)}{2} \right] \right)$$

$$\tau_{\mathrm{RD}}^{-1} = \frac{\gamma \mu_0 \eta Q}{2} M_z$$

$$\mathrm{M}_z = M_0 \; tanh \left(\tfrac{t-t_0}{\tau} - \log \left[\tan \tfrac{\theta(t_0)}{2} \right] \right)$$

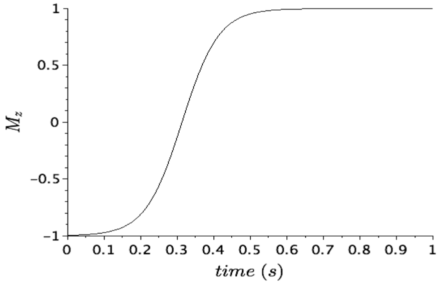

Analytical solutions exist for pure RD (no relaxation)

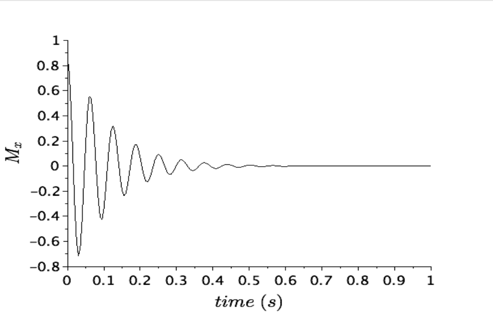

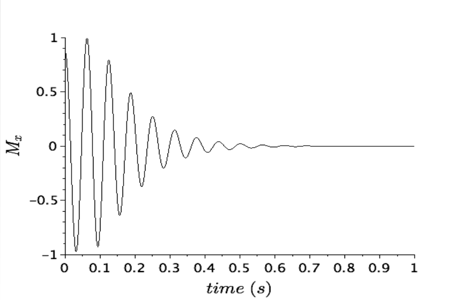

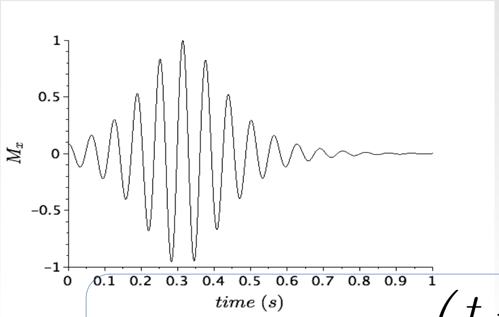

$$M_t = M_0\ sech\left(\frac{t - t_0}{\tau} - \log\left[\tan\frac{\theta(t_0)}{2}\right]\right)$$

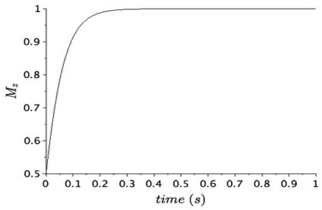

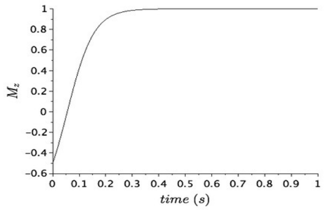

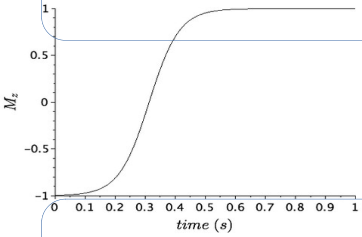

$$M_z = M_0\ tanh\left(\frac{t - t_0}{\tau} - \log\left[\tan\frac{\theta(t_0)}{2}\right]\right)$$

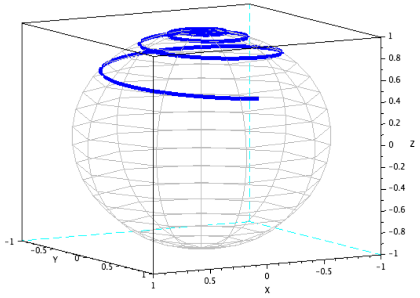

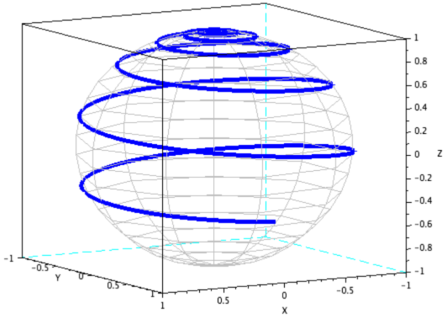

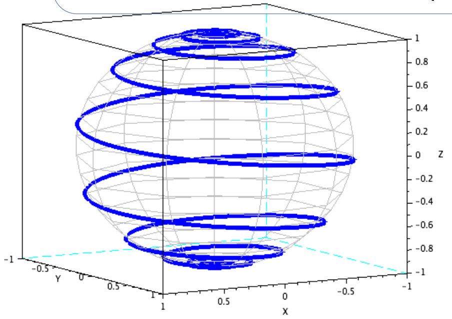

Motion on the Bloch Sphere (|M(t)| = constant)

Analytical solutions also exist for RD with pure T_2 relaxation

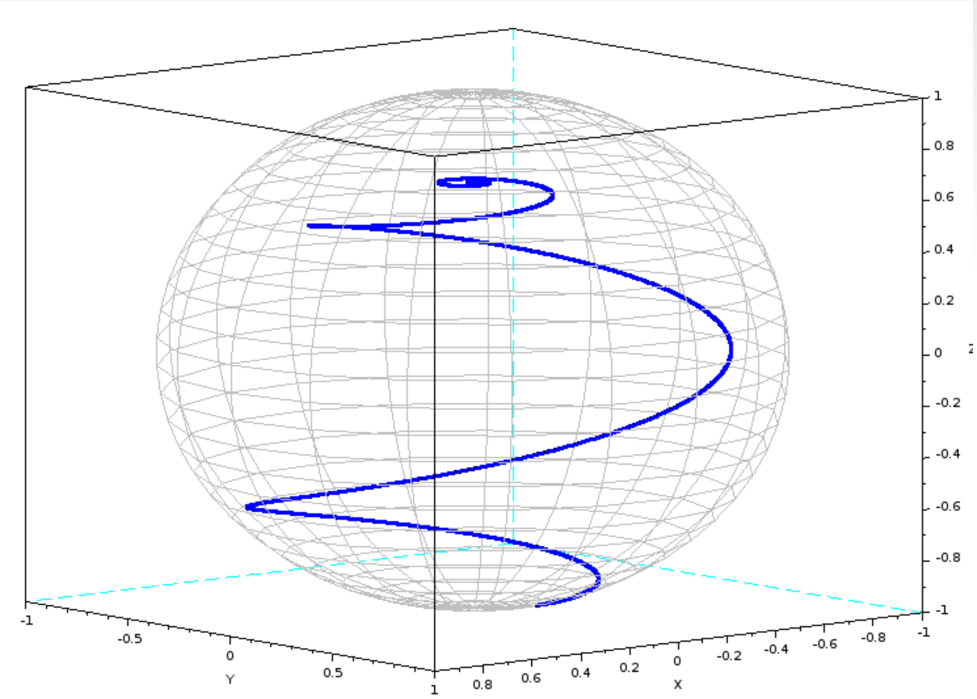

The dynamics is simple: a return to the equilibrium direction

In the absence of T1, the norm of the emagnetization vector is not restored to its equilibrium value

Study of the Maxwell-Bloch equation – a summary of possible situations

case $\omega_1 = 0$	Analytical	qualitative	numerical
No relaxation	yes	yes	yes
T_2	yes	yes	yes
T_2 , T_1	no	yes	yes

case $\omega_1 \neq 0$	Analytical	qualitative	numerical
No relaxation	yes	yes	yes
T_2	no	yes	yes
T_2 , T_1	no	no	yes

In all these situations, the dynamics is simple.

- What can make the dynamics more complex?

Antagonizing dissipation and energy loss to the coil yields richer dynamics

RD : the feedback field lags the transverse magnetization and rotate **m** towards +**z**

RD: $\psi = -\pi/2$

Equilibrium magnetization $\mathrm{m}_{0z}^{th} > 0$

Both lead the magnetization to the same equilibrium

- What if ψ is made *arbitrary*? If $\psi = +\pi/2$ the feedback field drives **m** to -**z**
- What if the stationary value m_0^{st} of is negative (magnetization pointing to -z)?
- Relaxation of m_z towards a time-varying value?

Each case corresponds to actual experimental situations, combined in the following equations :

$$\dot{m}_x = \delta m_y + \gamma G m_z (m_x \sin\psi - m_y \cos\psi) - \gamma_2 m_x$$

$$\dot{m}_y = -\delta m_x - \omega_1 m_z + \gamma G m_z (m_x \cos\psi) + m_y \sin\psi) - \gamma_2 m_y$$

$$\dot{m}_z = \omega_1 m_y - \gamma G \sin\psi (m_x^2 + m_y^2) - \gamma_z (m_z - m_{0z}^{th})$$

$$\dot{m}_{oz}^{th}(t) = -\gamma_{st}(m_{oz}^{th}(t) - m_0^{st})$$

Generalized feedback with arbitrary phase

Time-varying «stationary» m^{th}_{0z}

What magnetization dynamics do these equations predict ?

The example dynamics of “inverted” radiation damping: $\psi=+\pi/2$ and relaxation (towards equilibrium with longitudinal time T_1)

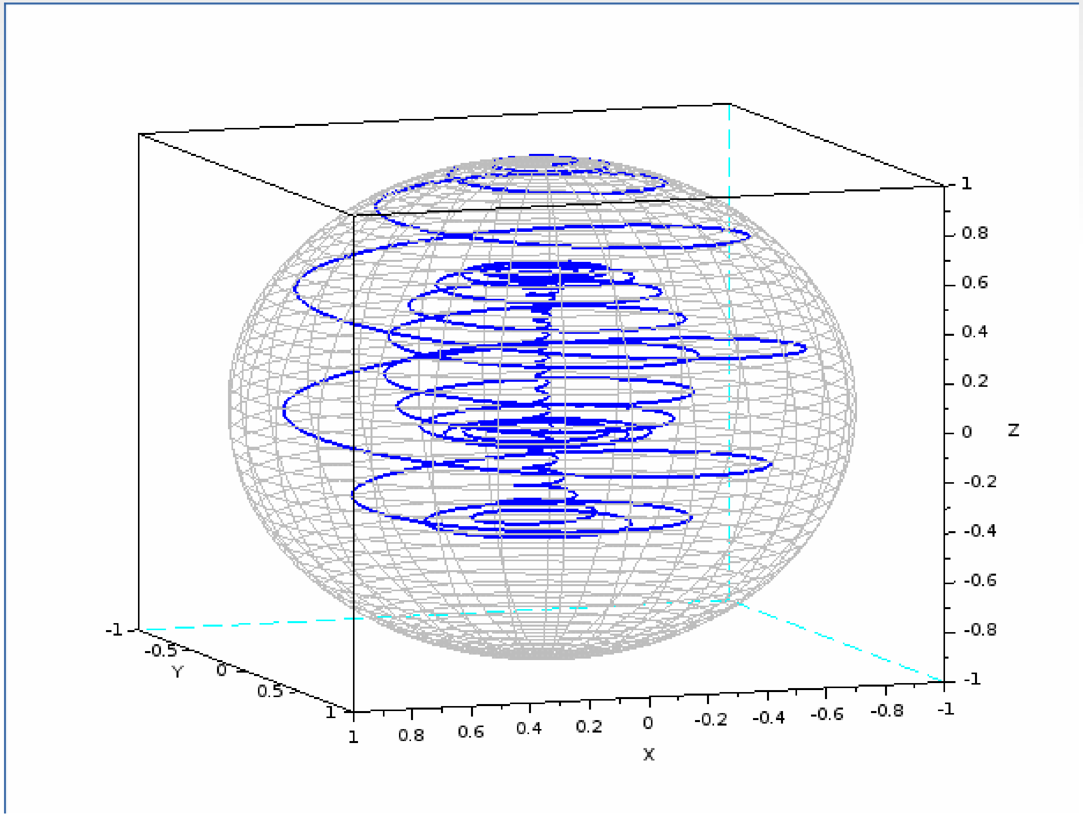

- These equations have additional dynamical content,
- But in general no analytical solution can be found

A qualitative analysis of the nonlinear Bloch-Maxwell equations ($\omega_1 = 0$)

Change of variables $\lambda = \gamma G$ $u = m_x^2 + m_y^2,\ m_z = z$ and $m_t = m_x + i m_y = \sqrt{u} e^{i\phi(t)}$

(change of variable only possible if $\omega_1 = 0$)

$$\begin{cases} \dot{u}(t) = 2(\lambda z(t) \sin\psi - \gamma_2) u(t) \\ \dot{z}(t) = -\lambda \sin\psi u(t) - \gamma_z (z(t) - w(t)) \\ \dot{w}(t) = -\gamma_{st} \left(w(t) - w^0\right) \\ \dot{\phi}(t) = -\delta + \lambda \cos\psi \ z \end{cases}$$

w^0 : equilibrium magnetization (thermal/stationnary)

Stationary solutions $\rightarrow$ Fixed points can be found *in particular cases*

$$F_1 = (0, w^0, w^0)$$

$\Rightarrow$ Thermal equilibrium

$$F_2 = \left(-\frac{\gamma_z}{\lambda \sin\psi}\left[\frac{\gamma_2}{\lambda \sin\psi} - w^0\right], \frac{\gamma_2}{\lambda \sin\psi}, w^0\right)$$

$\Rightarrow$ An in-plane component persists

Fixed point stability in the Radiation Damping case ($w^0 > 0, \ \sin\psi < 0$)
F_1 stable, F_2 unstable

$$F_2 = \left(-\frac{\gamma_z}{\lambda\sin\psi}\left[\frac{\gamma_2}{\lambda\sin\psi} - w^0\right], \frac{\gamma_2}{\lambda\sin\psi}, w^0\right)$$

$$\begin{bmatrix}\dot U\\ \dot Z\\ \dot W\end{bmatrix} = \begin{bmatrix} 0 & 2\lambda\sin\psi\, u^{st} & 0\\ -\lambda\sin\psi & -\gamma_z & \gamma_z\\ 0 & 0 & -\gamma_{st}\end{bmatrix}\begin{bmatrix}U\\ Z\\ W\end{bmatrix} + \begin{bmatrix}-2\lambda\sin\psi ZU\\ 0\\ 0\end{bmatrix}$$

$$x_0 = -\gamma_{st}$$

$$x_\pm = \frac{-\gamma_z \pm\sqrt{\Delta}}{2}, \ \Delta = \gamma_z(\gamma_z + 8\gamma_2 - 8\lambda w^0\sin\psi)$$

$\boxed{w^0\times\sin\psi < 0}$ $\Rightarrow \Delta >$ and $x_+ > 0, \ x_- < 0$

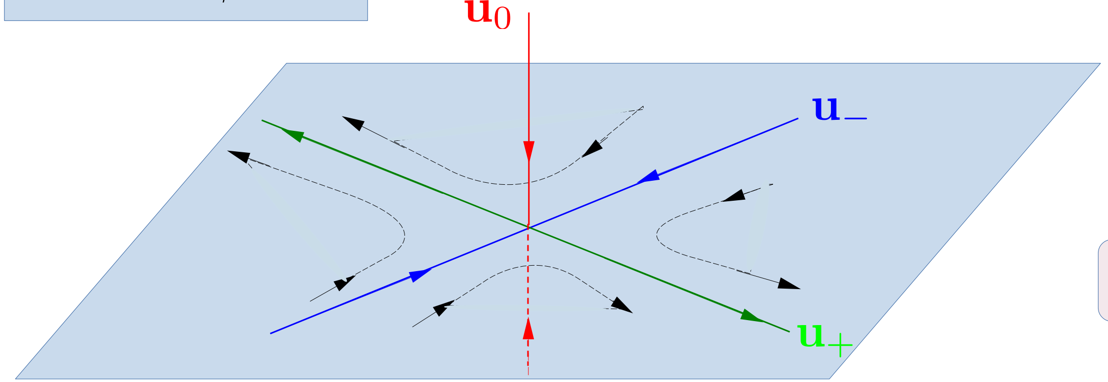

$$F_1 = (0, w^0, w^0)$$

$$\begin{bmatrix}\dot U\\ \dot Z\\ \dot W\end{bmatrix} = \begin{bmatrix} 2(\lambda\sin\psi - \gamma_2) & 0 & 0\\ -\lambda\sin\psi & -\gamma_z & \gamma_z\\ 0 & 0 & -\gamma_{st}\end{bmatrix}\begin{bmatrix}U\\ Z\\ W\end{bmatrix} + \begin{bmatrix}-2\lambda\sin\psi ZU\\ 0\\ 0\end{bmatrix}$$

$$x_0 = -\gamma_{st}$$
$$x_1 = -\gamma_z$$
$$x_2 = 2(\lambda\sin\psi w^0 - \gamma_2)$$

F_2 unstable

F_1 stable

Fixed point stability in the case $w^0 \times \sin\psi > 0$

$$F_2 = \left(-\frac{\gamma_z}{\lambda\sin\psi}\left[\frac{\gamma_2}{\lambda\sin\psi} - w^0\right], \frac{\gamma_2}{\lambda\sin\psi}, w^0\right)$$

$$\begin{bmatrix} \dot U \\ \dot Z \\ \dot W \end{bmatrix} = \begin{bmatrix} 0 & 2\lambda\sin\psi\, u^{st} & 0 \\ -\lambda\sin\psi & -\gamma_z & \gamma_z \\ 0 & 0 & -\gamma_{st} \end{bmatrix} \begin{bmatrix} U \\ Z \\ W \end{bmatrix} + \begin{bmatrix} -2\lambda\sin\psi ZU \\ 0 \\ 0 \end{bmatrix}$$

$$\begin{aligned} x_0 &= -\gamma_{st} \\ x_\pm &= \frac{-\gamma_z \pm \sqrt{\Delta}}{2}, \ \Delta = \gamma_z(\gamma_z + 8\gamma_2 - 8\lambda w^0 \sin\psi) \end{aligned}$$

$$F_1 = (0, w^0, w^0)$$

$$\begin{bmatrix} \dot U \\ \dot Z \\ \dot W \end{bmatrix} = \begin{bmatrix} 2(\lambda\sin\psi - \gamma_2) & 0 & 0 \\ -\lambda\sin\psi & -\gamma_z & \gamma_z \\ 0 & 0 & -\gamma_{st} \end{bmatrix} \begin{bmatrix} U \\ Z \\ W \end{bmatrix} + \begin{bmatrix} -2\lambda\sin\psi ZU \\ 0 \\ 0 \end{bmatrix}$$

$$\begin{aligned} x_0 &= -\gamma_{st}, \quad x_1 = -\gamma_z \\ x_2 &= 2(\lambda\sin\psi w^0 - \gamma_2) \end{aligned}$$

✓ $0 < \lambda\sin\psi w^0 < \gamma_2 \Rightarrow x_2 < 0$ and: F_1 stable F_2 unstable

✓ $\lambda\sin\psi w^0 - \gamma_2 > 0 \Rightarrow x_2 > 0$ and: F_1 unstable F_2 stable

When $\Delta < 0 \Rightarrow F_2$ stable focus

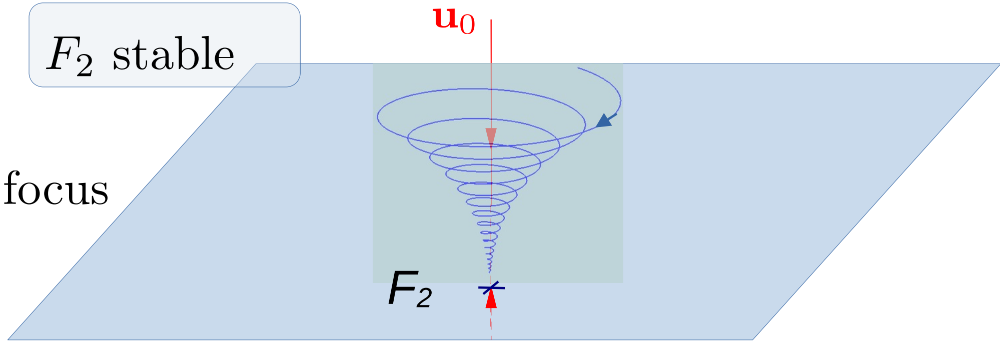

Sustained masers are predicted when F2 is a stable focus

✓ $\lambda \sin\psi w^0 - \gamma_2 > 0 \Rightarrow x_2 > 0$ and: F_1 unstable F_2 stable

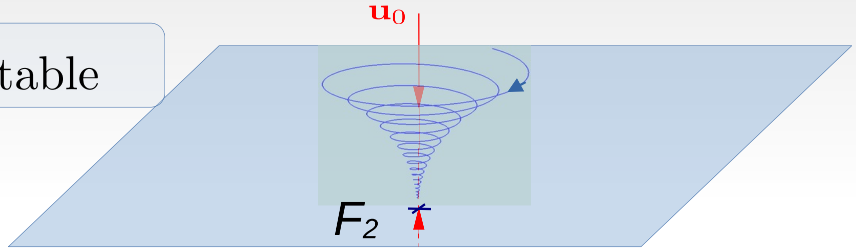

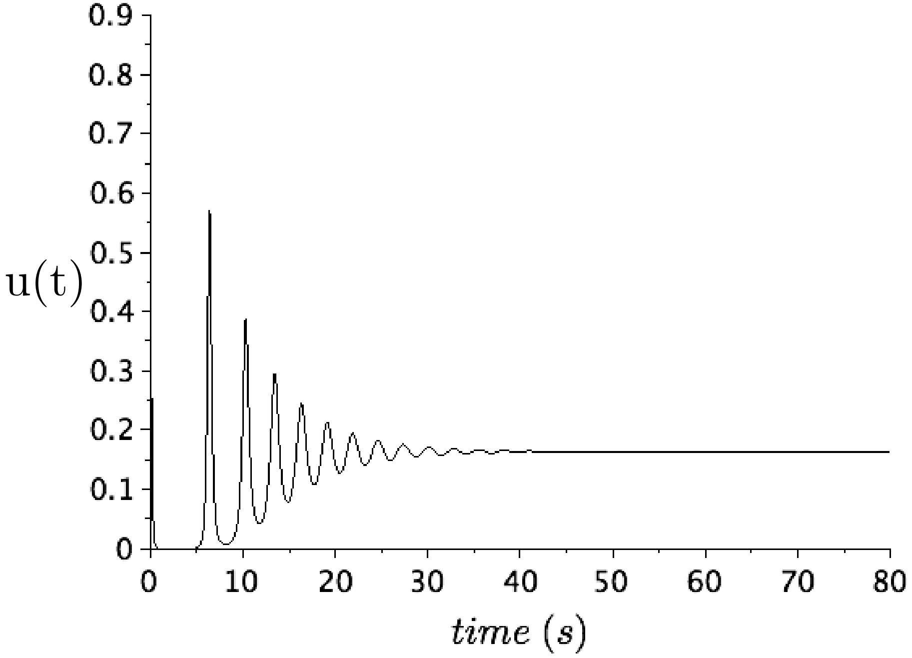

When $\Delta < 0 \Rightarrow F_2$ stable focus

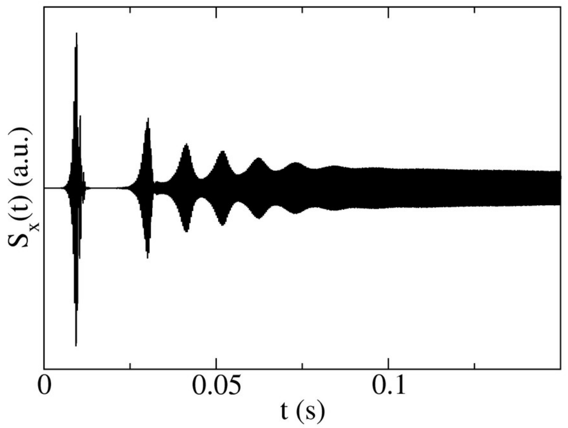

This can be observed in DNP experiments

Numerical investigations of the nonlinear Bloch equations in the presence of ω_1: Instability and chaos

When a constant radiofrequency field is applied,
much richer dynamics is predicted by the equations

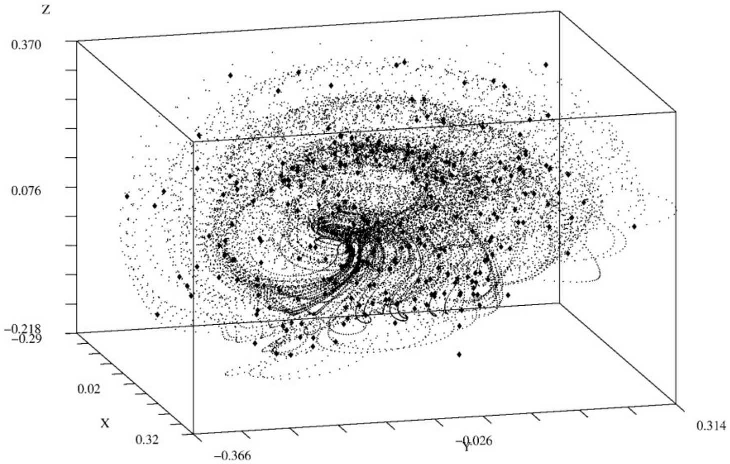

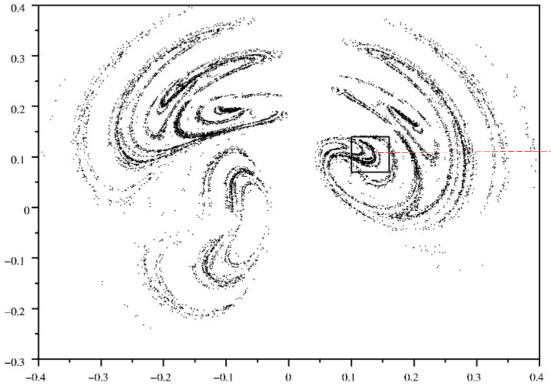

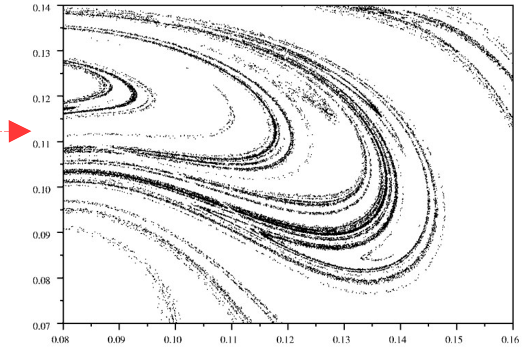

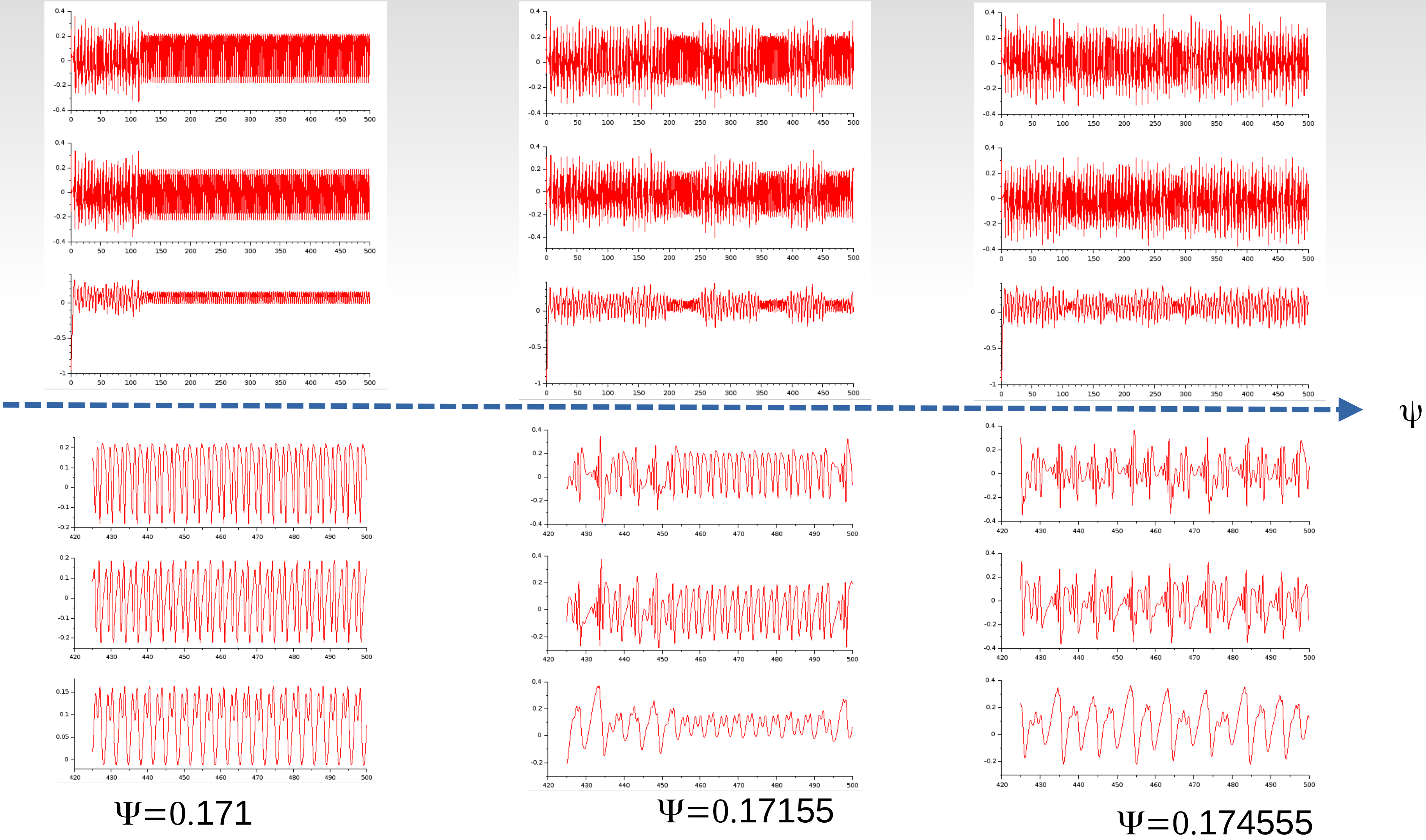
ψ
Ψ=0.171
Ψ=0.17155
Ψ=0.174555

Transition to chaos of the nonlinear Bloch equations: period doubling and intermittency

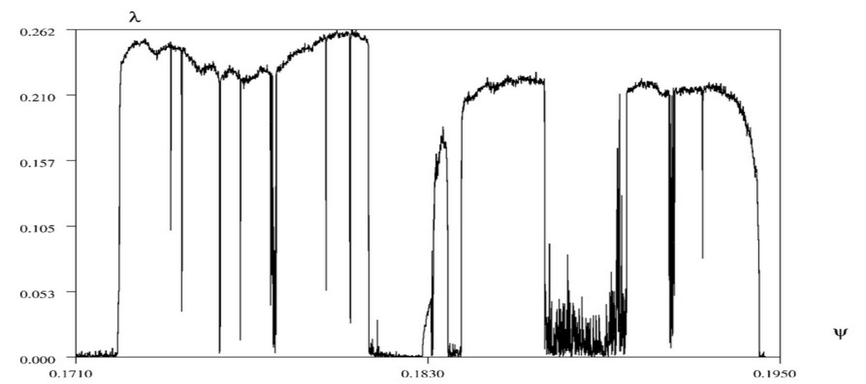

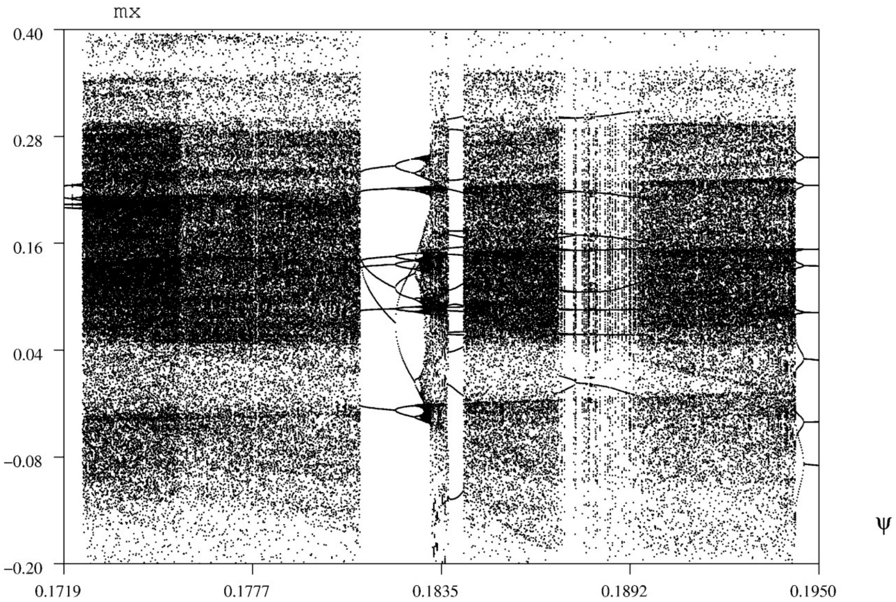

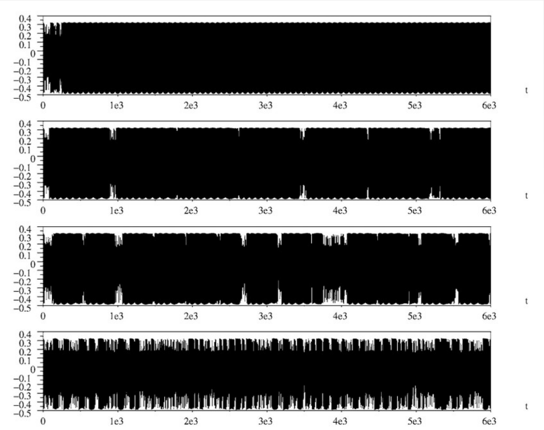

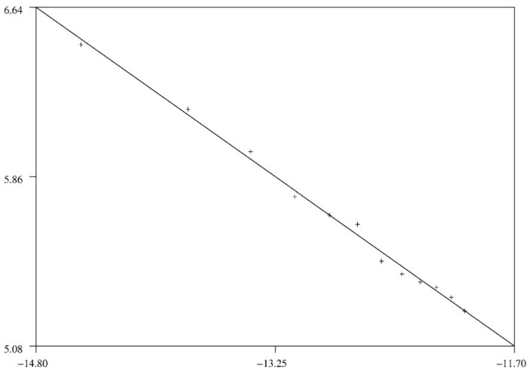

Back to experiments...

Liquid state experiments
controlled radiation damping

- ambient temperature
- Long T2 and narrow line width (~ Hz)
- No efficient dipolar interactions between spins (motional averaging)
- « Large » magnetization ; low polarization ~ 5.10^{-5}

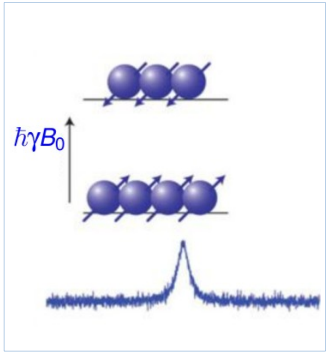

Solid state DNP experiments

- low temperature DNP (~ 1,2 K)
- Very short T2 and broad lines (~ 50 kHz)
- Strong local dipolar interactions
- «Huge» magnetization (hyperpolarization up to 80-90 %)

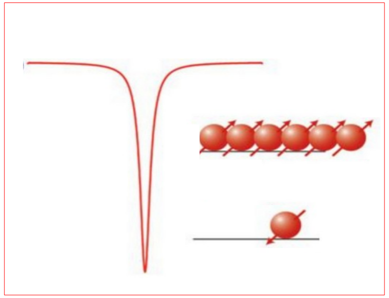

Low Temperature Dynamic Nuclear Polarization experiments

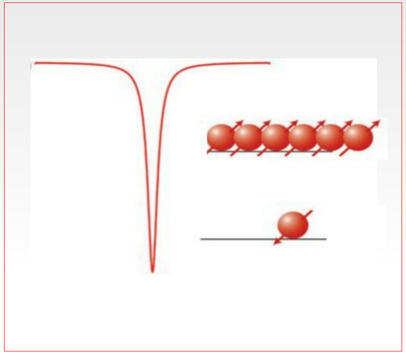

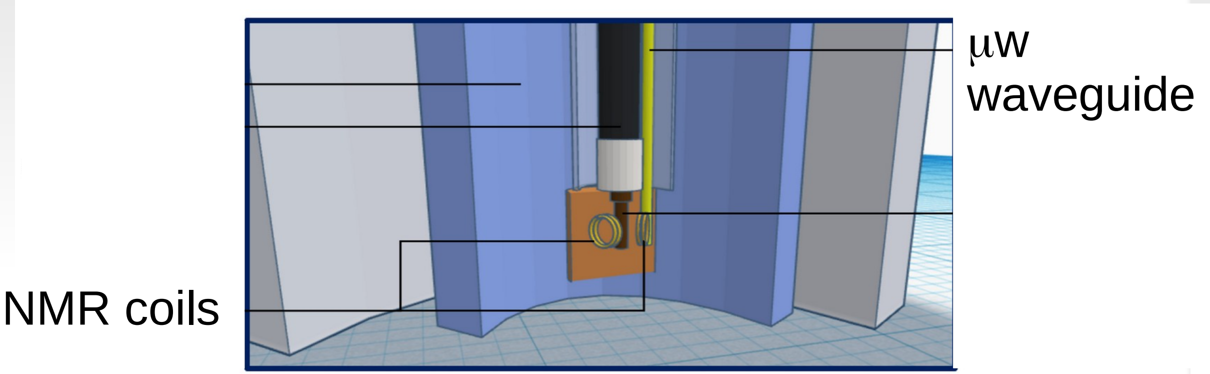

Liquid helium bath at T ~ 1,2 K

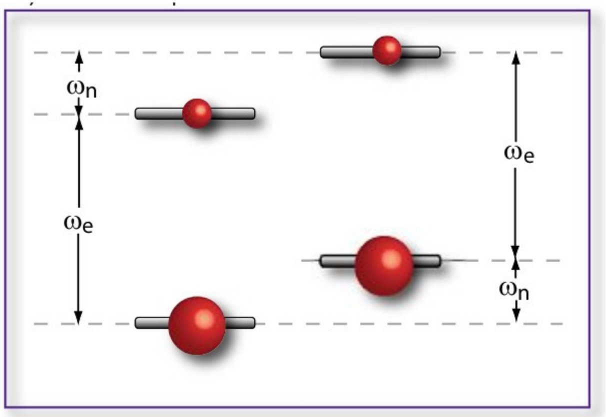

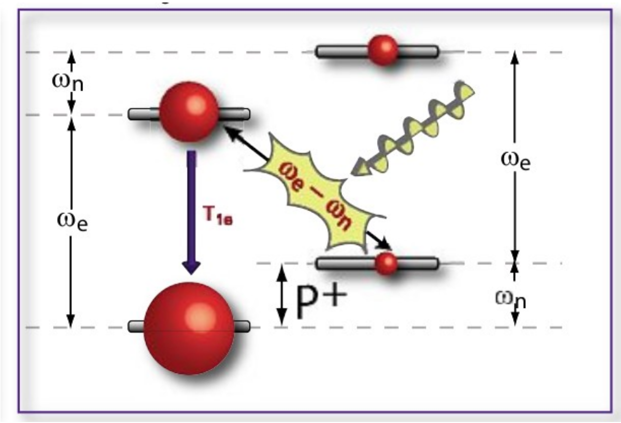

$$\gamma_e/\gamma_n \sim 660$$

e- spins : ~100 % polarized at 1.2 K

One mechanism of Dynamic Nuclear Polarization: the solid effect

Low Temperature Dynamic Nuclear Polarization experiments

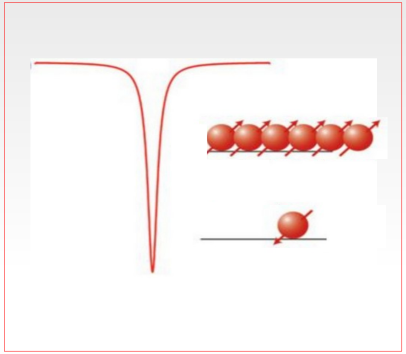

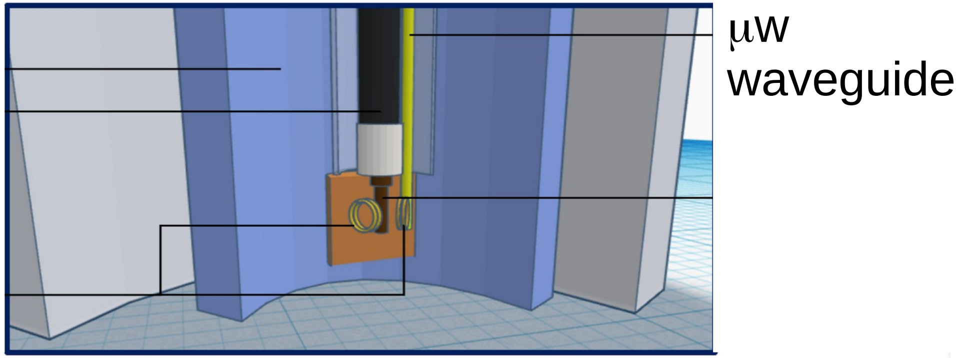

Liquid helium bath at T ~ 1,2 K

- Negative *hyperpolarization*: $m_0^{st} < 0$
- « normal » feedback: $\psi = \pi/2, \; \sin\psi = -1$

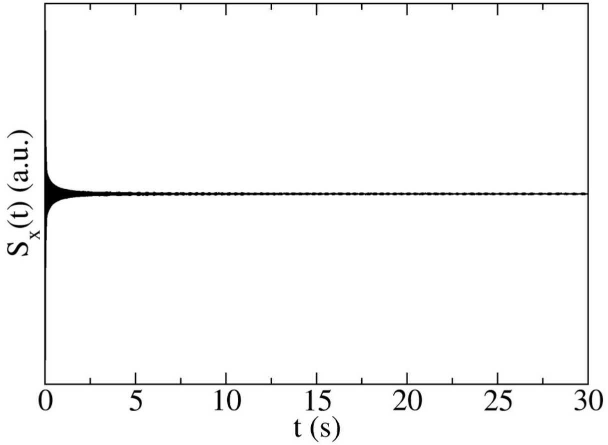

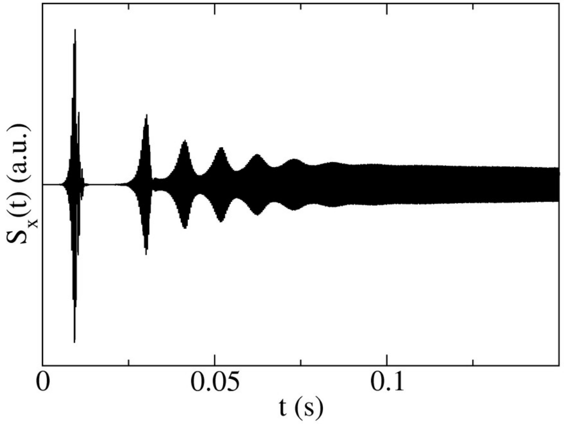

Time-delayed representation of the DNP signal *envelope*

- In NMR experiments, only the transverse components of m are detected

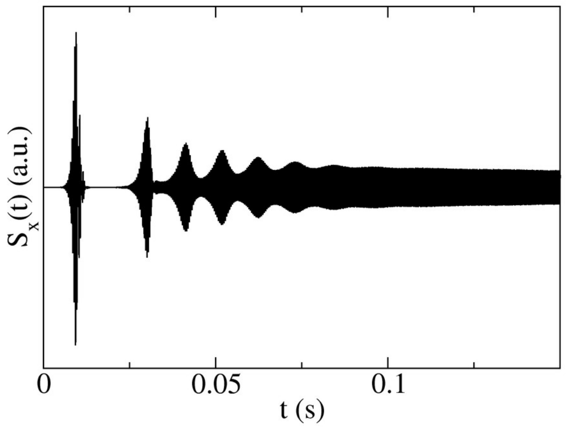

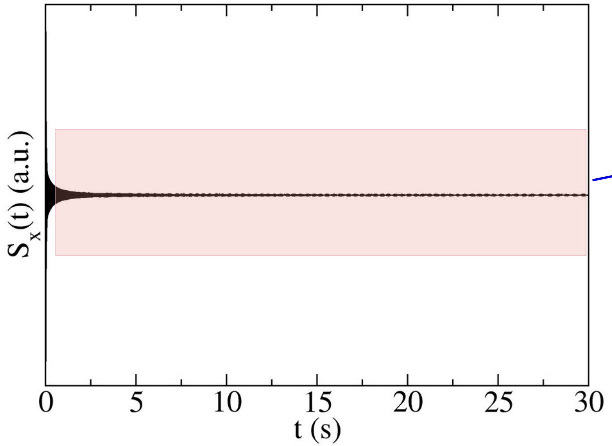

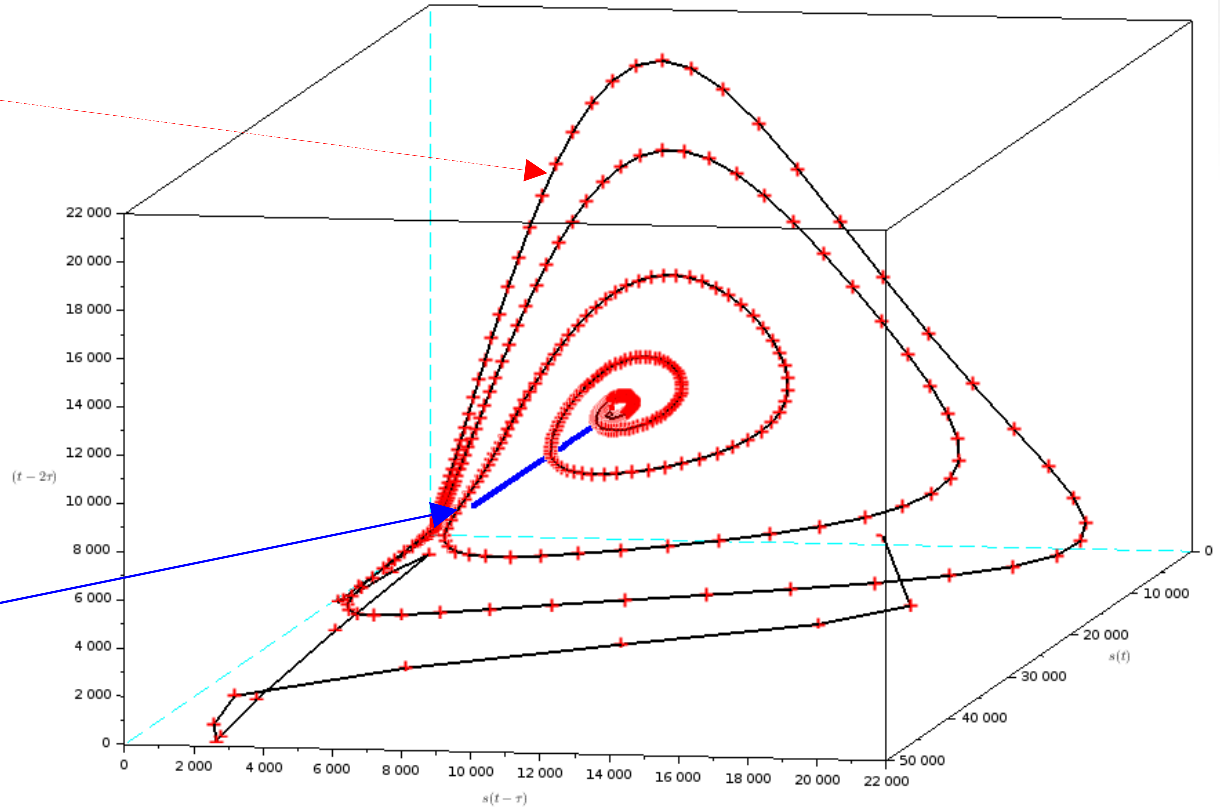

$$(s(t), s(t-\tau), s(t-2\tau))$$

Experimental masers can be qualitatively fitted by the extended Maxwell-Bloch equations

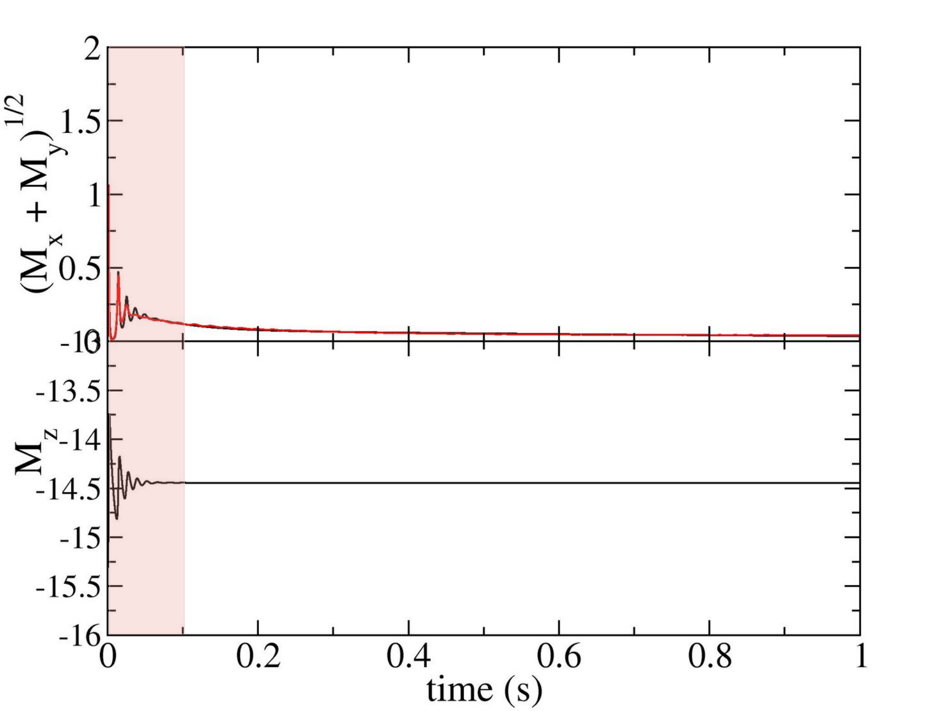

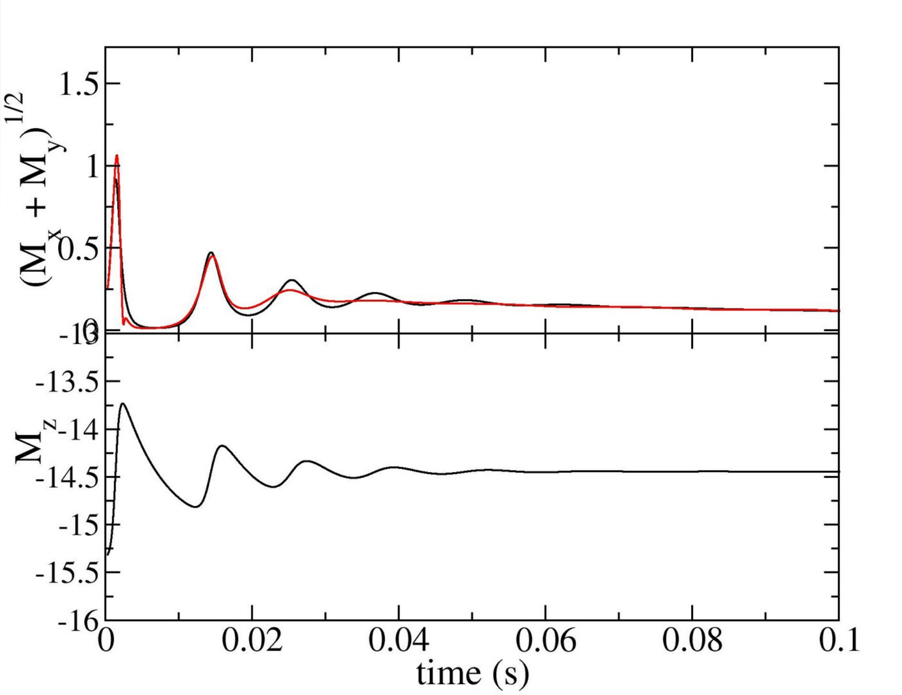

$$\dot{m}_x = \delta m_y - \gamma G m_z m_x - \gamma_2 m_x$$

$$\dot{m}_y = -\delta m_x - \gamma G m_z m_y - \gamma_2 m_y$$

$$\dot{m}_z = \gamma G(m_x^2 + m_y^2) - \gamma_z(m_z - m_{0z}^{th})$$

$$\dot{m}_{oz}^{th}(t) = -\gamma_{st}(m_{oz}^{th}(t) - m_0^{st})$$

negative polarization DNP $m_0^{st} < 0_x$

- m_x and m_y are detected
- m_z is only *reconstructed*

Different experimental conditions give different observations

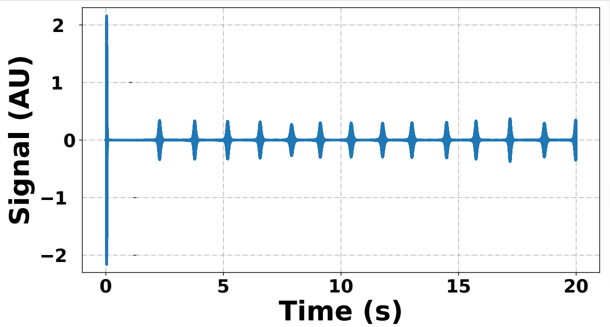

- sustained signal bursts upon μwave irradiation (repolarization)
- hour-long observations
- **no damping of the maser bursts**

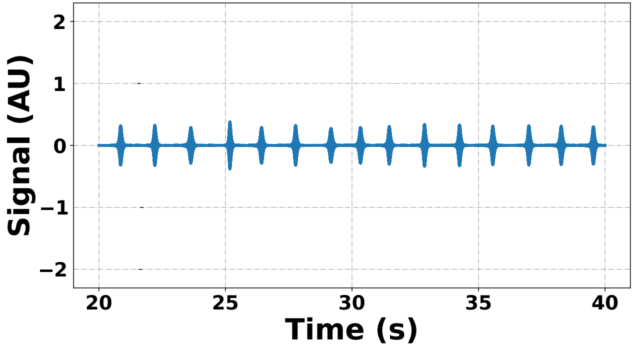

- convergence to a regular, ~ periodic signal
- with a few irregular bursts

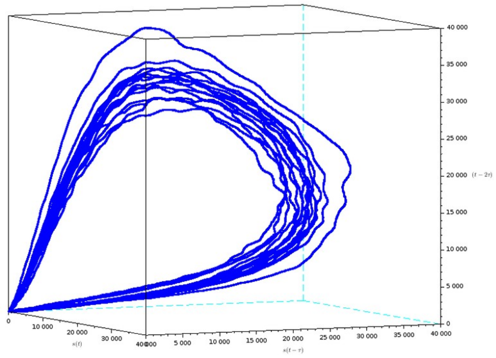

$$(s(t), s(t-\tau), s(t-2\tau))$$

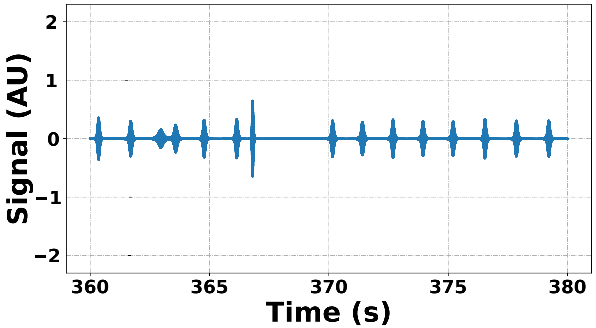

Dynamics seem to converge to a limit cycle
… not compatible with the extended MB equations

Similar observation *in solution, at ambient temperature* with electronic control of RD

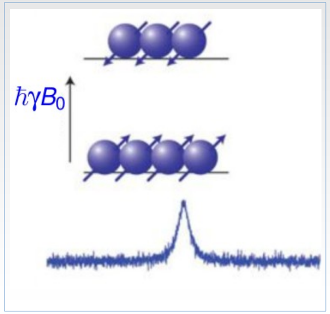

- Thermal (positive) polarization $m_0^{st} > 0$
- controlled feedback: $\sin\psi > 0$

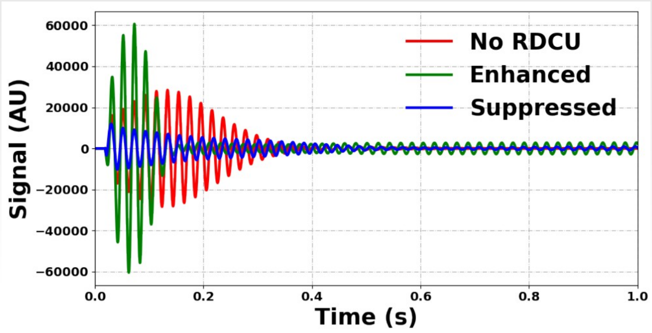

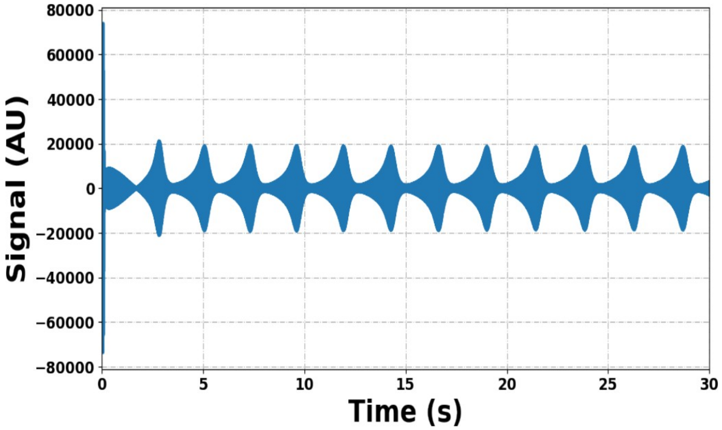

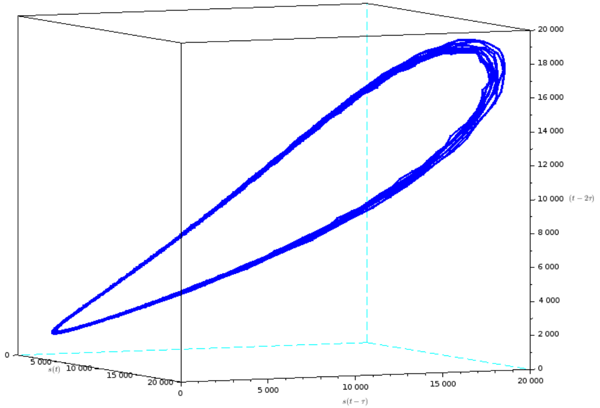

$$(s(t), s(t-\tau), s(t-2\tau))$$

- ~ periodic signal
- no damping of the signal bursts

Dynamics seem to converge to a limit cycle
… not compatible with the MB equations

The failure of the model is due to a distribution of Larmor frequencies in the sample

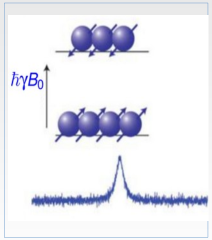

- In solution, the main source of distribution of Larmor frequencies is the inhomogeneity of the static field
- At different locations in the sample, the spins have a Larmor frequency offset δω
- The feedback field is thus local, but each spin feels the cumulative effect of the local feedback fields
- The system is high-dimensional...

$$\mathbf{B}_{FB}(\delta\omega) = \lambda \mathbf{m}_t(\delta\omega;t)e^{-i\psi} \qquad \mathbf{B}_{FB} = \int \mathbf{B}_{FB}(\delta\omega)d(\delta\omega)$$

$$\mathbf{B}_{FB} = \lambda \begin{pmatrix} \sin\psi \int_{-\infty}^{\infty} m_y(\delta\omega)d(\delta\omega) + \cos\psi \int_{-\infty}^{\infty} m_x\delta\omega)d(\delta\omega) \\ -\sin\psi \int_{-\infty}^{\infty} m_x(\delta\omega)d(\delta\omega) + \cos\psi \int_{-\infty}^{\infty} m_y\delta\omega)d(\delta\omega) \\ 0 \end{pmatrix}$$

Failure of the simple Maxwell-Bloch equations is due to a distribution of Larmor frequencies in the sample

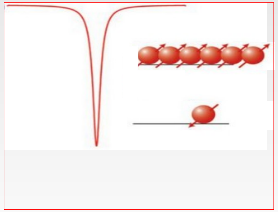

- DNP-polarized spins generate large dipolar fields

$$\mathbf{B}_d(\mathbf{r}_i) = \frac{\mu_0}{4\pi}\sum_j \frac{1-3\cos^2\theta_{ij}}{2\left|\mathbf{r}_i-\mathbf{r}_j\right|^3} \times \left[3M_z(\mathbf{r}_j)\,\hat{\mathbf{z}} - \mathbf{M}(\mathbf{r}_j)\right]$$

- Average dipolar field: $\omega_{dip} \propto m_0^{st}$
- The evolution depends on the ratio ω_{dip}/ω_{rd}
- The spread of the z- component is the crucial ingredient

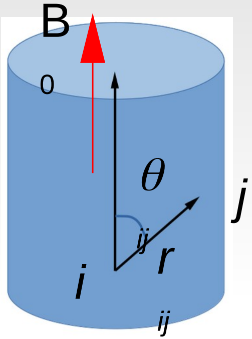

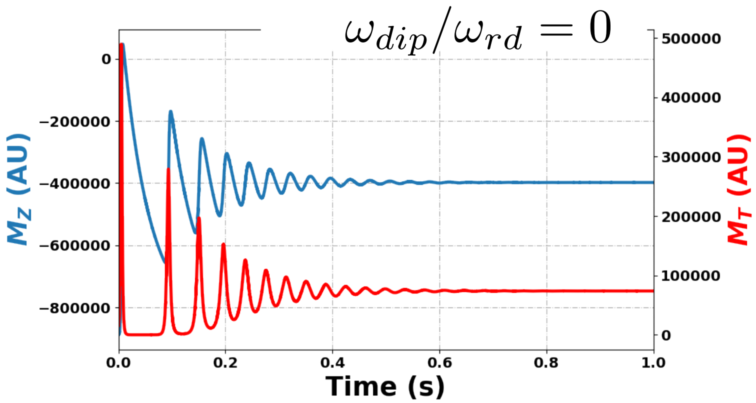

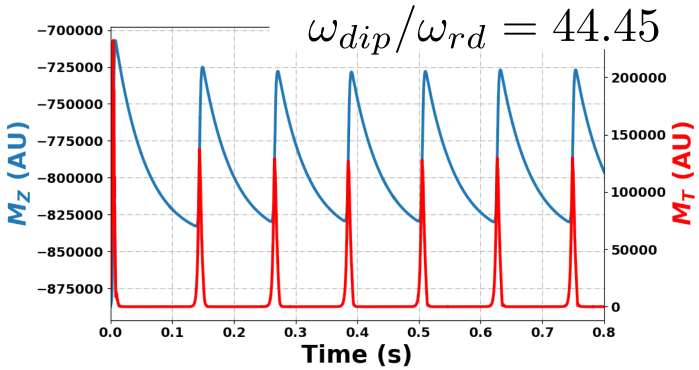

Conclusions: chaotic signals in solution and in a hyperpolarized frozen solution

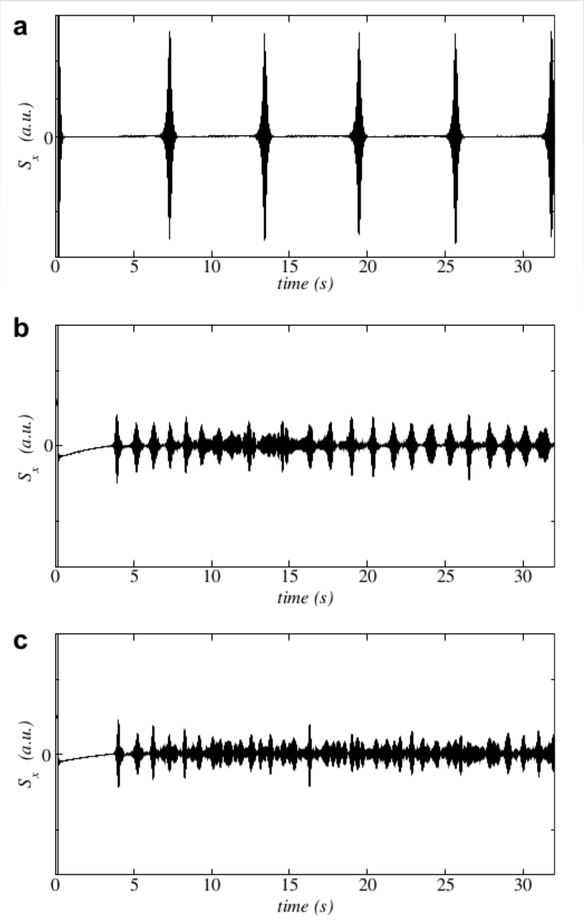

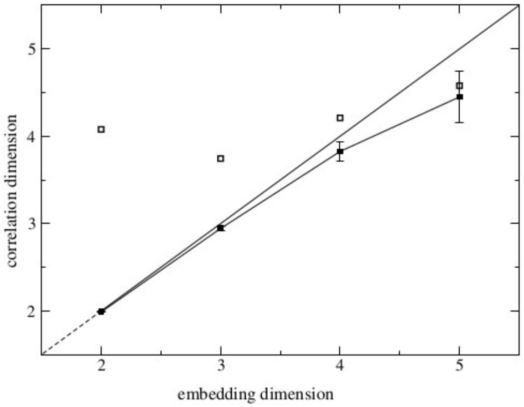

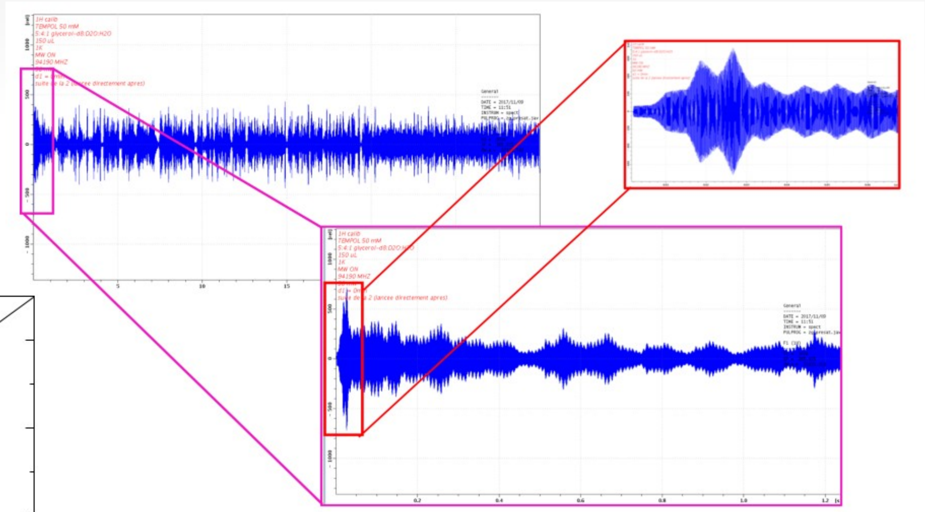

Chaotic signal in a DNP-polarized sample

Chaotic signal in solution

Thanks!

Vineeth Thalakottoor (LBM, ENS/CNRS/SU)

Alain Louis-Joseph (LPMC, EP/CNRS)

Projet DynNonlinPol